Acta Crystallographica Section A
**Foundations of Crystallography**
ISSN 0108-7673

Received 18 January 2002
Accepted 21 March 2002



# Group-theoretical and geometrical considerations of the phase transition between the high-temperature polymorphs of quartz and tridymite

**H. Sowa[a] and E. Koch[b]***

[a]Institut für Angewandte Geowissenschaften, Allgemeine und Angewandte Mineralogie, Technische Universität BH1, Ernst-Reuter-Platz 1, D-10587 Berlin, Germany, and [b]Institut für Mineralogie, Petrologie und Kristallographie der Philipps-Universität Marburg, Hans-Meerwein-Strasse, D-35032 Marburg, Germany. Correspondence e-mail: kochelke@mailer.uni-marburg.de

A model was derived for the temperature-dependent phase transition between the high-temperature polymorphs of quartz ($P6_422$) and tridymite ($P6_3/mmc$). Only the Si framework is considered, and the transformation can be described as a deformation of a homogeneous sphere packing with three contacts per sphere (type 3/10/$h$1) in the common subgroup $P6_122$ of $P6_422$ and $P6_3/mmc$. The proposed model guarantees the three-dimensional connection of the crystal structure during the whole transformation process.

## 1. Introduction

Dependent on temperature and pressure, silica, $SiO_2$, exhibits several polymorphs. At ambient pressure and 846 K, it undergoes a phase transition from the low- ($\alpha$) to the high-temperature ($\beta$) form of quartz. Between 1130 and 1743 K, the high-temperature polymorph of tridymite is the stable phase, and above 1743 K up to the melting temperature of 1986 K, the high-temperature modification of cristobalite exists (*cf. e.g.* Putnis, 1992). In all these phases, the silicon atoms are fourfold coordinated by oxygen atoms. The phase transition from $\alpha$- to $\beta$-quartz is displacive and can easily be described using group–subgroup relations. As the tetrahedral linkage is different in quartz, tridymite and cristobalite, during the transformations between these phases bonds have to be broken and, therefore, the phase transitions are reconstructive.

In a recent paper, Leoni & Nesper (2000) proposed a mechanism for the phase transition between the high-temperature polymorphs of quartz and tridymite. For both structures, the authors calculated periodic equi-surfaces (*cf.* von Schnering & Nesper, 1991) using the Fourier summation over a small set of specifically selected structure factors as the respective basis functions. Then, the four-coordinated silicon network lies on one side of the resulting equi-surface, *i.e.* within one of the two labyrinths, or – in other words – the surface envelops the silicon network. Leoni & Nesper (2000) modelled the phase transition within a common supercell of quartz and tridymite. They assumed that the **a** and **c** axes of both structures run parallel and that the $c$ lattice parameter of the intermediate arrangement is approximately quadruple that of quartz and triple that of tridymite. Equi-surfaces for the intermediate structures were calculated by weighted addition of the basis functions of quartz and tridymite. Their investigation showed that one connection per Si atom has to be broken leading to a three-coordinated Si network in the intermediate arrangement. By this method only the topology of the silicon network can be modelled.

For the transition between the high-temperature polymorphs of tridymite and cristobalite, a pathway was proposed by Sowa & Koch (2001). Symmetry relations between diamond and lonsdaleite were investigated and a possible transition model for the phase transformation was described by means of sphere-packing deformations. Since the arrangements of Si atoms in high-temperature tridymite and high-temperature cristobalite correspond to the carbon configurations in lonsdaleite and diamond, respectively, a related model could be derived for the transition from high-temperature tridymite to high-temperature cristobalite. The transformation was described in space group *Pnna*, where the intermediate Si arrangement corresponds to a homogeneous sphere packing with three contacts per sphere. The movement of the O atoms was expected to be similar to that described by Leoni & Nesper (2000) for the transition between quartz and tridymite.

Analogously, in the present paper a transformation mechanism is described for the phase transition between $\beta$-quartz and high-temperature tridymite using group-theoretical considerations and sphere-packing deformations. It is not the aim of the present paper to contribute to the discussions on the existence or non-existence of a stable high-temperature modification of tridymite. As a phase transition from high-temperature tridymite into $\beta$-quartz apparently can take place at least in the presence of certain impurities (*cf. e.g.* Ray, 1947; Flörke, 1959; Flörke & Langer, 1972), it seems worthwhile to compare the recently published model (Leoni & Nesper, 2000) with a mechanism based on group-theoretical considerations.

## 2. Symmetry relations between the high-temperature polymorphs of quartz and tridymite

The connectivity and the topological properties of the silica structures may be discussed exclusively on the basis of the silicon positions. For many purposes, it is not necessary to consider the exact positions of the oxygen atoms, and so only the silicon frameworks are considered in the following investigations. In both structures, the Si atoms correspond to homogeneous sphere packings with four contacts per sphere.

$\beta$-Quartz crystallizes in space group $P6_422$ (or in the enantiomorphic group $P6_222$). The Si arrangement corresponds to a homogeneous sphere packing of type 4/6/$h$1 (Fischer & Koch, unpublished material; *cf.* Fischer & Koch, 1994). The atoms occupy *e.g.* the Wyckoff position 3($d$) 222 $\frac{1}{2},\frac{1}{2},\frac{1}{6}$. Each silicon atom is surrounded by four other Si atoms forming an orthorhombically distorted tetrahedron with four equal distances from the central atom to the vertices. If the axial ratio $c/a$ equals $\frac{3}{4}\times 2^{1/2}\simeq 1.0607$, a configuration with minimal density, *i.e.* with maximal volume, is obtained. With $c/a\approx 1.09$ (Kihara, 1990), the axial ratio of $\beta$-quartz deviates only slightly from this ideal value.

The space group of tridymite is $P6_3/mmc$. Here, the silicon atoms are arranged just as the carbon atoms in lonsdaleite. They are located at position 4($f$) $3m$. $\frac{2}{3},\frac{1}{3},z$ with $z\approx -0.062$ (Kihara, 1978) and correspond to a homogeneous sphere packing of type 4/6/$h$2 (Sowa, 2001; Sowa & Koch, 2001). In the ideal atomic arrangement, each silicon atom has four other Si neighbours forming an undistorted tetrahedron. It is obtained for $z=-\frac{1}{16}=-0.0625$ and for the axial ratio $c/a=\frac{2}{3}\times 6^{1/2}\simeq 1.6330$, which agrees quite well with the observed value $c/a\approx 1.64$.

As for the phase transformation between diamond and lonsdaleite (Sowa & Koch, 2001), a transition model was derived that retains the three-dimensional connection of the structure. It was assumed that during the transition all Si atoms remain symmetrically equivalent, that only one contact per Si atom is lost, and that the intermediate silicon arrangement can be described by a homogeneous sphere packing with three contacts per sphere. The only lattice complex that allows such a transformation corresponds to the general position 12($c$) of $P6_122$ (or $P6_522$). Here, the idealized silicon configuration of $\beta$-quartz is found with $c/a=3\times 2^{1/2}\simeq 4.2426$, *e.g.* at $x=\frac{1}{2}$, $y=\frac{1}{2}$, $z=\frac{7}{24}\simeq 0.29167$, whereas the undistorted lonsdaleite arrangement occurs with $c/a=2\times 6^{1/2}\simeq 4.8990$, *e.g.* at $x=\frac{2}{3}$, $y=\frac{1}{3}$, $z=\frac{5}{16}\simeq 0.3125$ (*cf.* Fig. 1).

**Table 1**
Symmetry operations and coordinates of neighbouring points that may give rise to sphere contacts if the original sphere is located in the interior or at the boundary of the parameter field of type 3/10/$h$1.

| Neighbour | Coordinates | Symmetry operation |
|---|---|---|
| *A* | $1-x,-x+y,\frac{2}{3}-z$ | $2_1$ ($\frac{1}{2}$, $y$, $\frac{1}{3}$) |
| | $1-x,1-x+y,\frac{2}{3}-z$ | |
| *B* | $1-x+y,y,\frac{1}{2}-z$ | 2 ($\frac{1}{2}+x$, $2x$, $\frac{1}{4}$) |
| *C* | $-x+y,y,\frac{1}{2}-z$ | 2 ($x$, $2x$, $\frac{1}{4}$) |
| *D* | $2-x,1-x+y,\frac{2}{3}-z$ | 2 (1, $y$, $\frac{1}{3}$) |
| *E* | $1-y,1-x,\frac{5}{6}-z$ | 2 ($1+x$, $-x$, $\frac{5}{12}$) |
| *F* | $y,1-x+y,-\frac{1}{6}+z$ | $6_1$ (1, 1, $z$) |
| | $1+x-y,x,\frac{1}{6}+z$ | |
| *G* | $y,-x+y,-\frac{1}{6}+z$ | $6_1$ (0, 0, $z$) |
| | $x-y,x,\frac{1}{6}+z$ | |
| *H* | $\pm 1+x,y,z$ | $t$ ($\pm 1$, 0, 0) |
| | $x,\pm 1+y,z$ | $t$ (0, $\pm 1$, 0) |
| | $\pm 1+x,\pm 1+y,z$ | $t$ ($\pm 1$, $\pm 1$, 0) |
| *I* | $2-x+y,y,\frac{1}{2}-z$ | 2 ($1+x$, $2x$, $\frac{1}{4}$) |
| *J* | $-x,-x+y,\frac{2}{3}-z$ | 2 (0, $y$, $\frac{1}{3}$) |
| *K* | $-y,-x,\frac{5}{6}-z$ | 2 ($x$, $-x$, $\frac{5}{12}$) |
| *L* | $1+y,-x+y,-\frac{1}{6}+z$ | $6_1$ (0, $-1$, $z$) |
| | $-1+x-y,-1+x,\frac{1}{6}+z$ | |
| *M* | $1+y,1-x+y,-\frac{1}{6}+z$ | $6_1$ (1, 0, $z$) |
| | $x-y,-1+x,\frac{1}{6}+z$ | |
| *N* | $x-y,-y,1-z$ | 2 ($x$, 0, $\frac{1}{2}$) |
| *O* | $y,x,\frac{1}{3}-z$ | 2 ($x$, $x$, $\frac{1}{6}$) |
| *P* | $1+y,-1+x,\frac{1}{3}-z$ | 2 ($1+x$, $x$, $\frac{1}{6}$) |

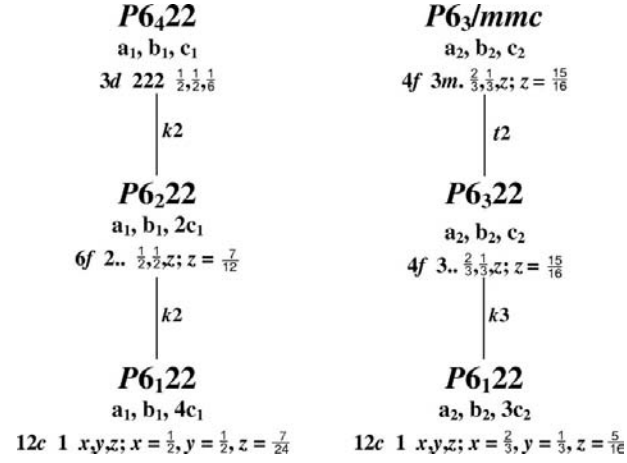


**Figure 1**
Symmetry relation between the crystal structures of the high-temperature polymorphs of quartz and tridymite. The transition from $P6_422$ to $P6_222$, as shown in the diagram, requires an origin shift by (0, 0, $-1$) referred to the basis of $P6_422$.

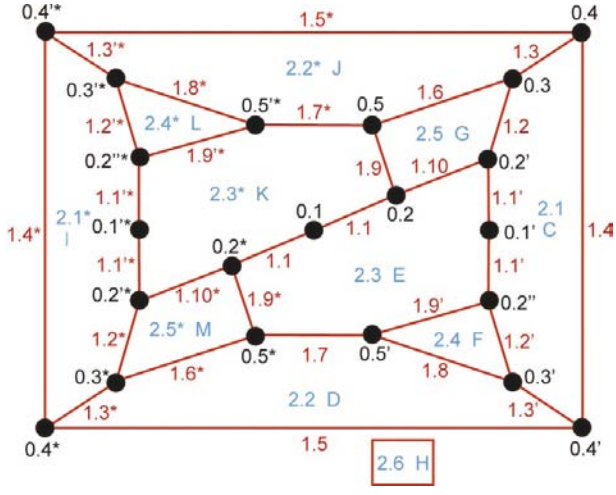


**Figure 2**
Sphere packings in the surroundings of 3/10/$h$1.

The three-coordinated sphere packing of the intermediate configuration belongs to type 3/10/*h*1. It can be realized with highest symmetry in $P6_222$ 6(*f*) (*cf.* Koch & Fischer, 1995).

## 3. Sphere packings in the surroundings of 3/10/*h*1

In the following, each sphere-packing type is designated by a symbol *k*/*m*/*hn* as was first introduced by Fischer (1971): *k* means the number of contacts per sphere, *m* is the length of the shortest mesh within the sphere packing, *h* indicates that the hexagonal/trigonal crystal family is the highest one for a sphere packing of that type, and *n* is an arbitrary number.

In order to generate different sphere packings in the general position 12(*c*) of $P6_122$, four parameters may be varied: the three positional parameters $x, y, z$ and the axial ratio $c/a$. Sphere packings of type 3/10/*h*1 occur if a reference sphere with centre at $x, y, z$ has three equidistant and symmetrically equivalent neighbours *e.g.* at $1-x, -x+y, \frac{2}{3}-z$; $1-x, 1-x+y, \frac{2}{3}-z$; and $1-x+y, y, \frac{1}{2}-z$. Equating the squared distances from the original sphere to the neighbouring ones yields the sphere-packing condition for 3/10/*h*1:

$$(x^2+y^2-4xy-x+2y)a^2+(\tfrac{2}{3}z-\tfrac{7}{36})c^2=0. \qquad (1)$$

The parameter region of 3/10/*h*1 in $P6_122$ has three degrees of freedom and may be visualized as a three-dimensional polyhedron in the four-dimensional parameter space. In Fig. 2, it is schematically represented by the Schlegel diagram of a polyhedron with 11 faces, 30 edges and 21 vertices. The interior of this polyhedron corresponds to the parameter region of type 3/10/*h*1, whereas its faces, edges and vertices belong to the adjacent parameter regions of sphere-packing types with contact numbers higher than three: 11 regions with two degrees of freedom (2.1 to 2.5), 30 with one (1.1 to 1.10) and 21 with no (0.1 to 0.5) degree of freedom. The parameter region of 3/10/*h*1 and, consequently, the Schlegel diagram show twofold rotation symmetry caused by the rotation $2(\frac{1}{2},0,z)$ belonging to the Euclidean normalizer $N_E(P6_122) = P6_222$ $(\mathbf{a}, \mathbf{b}, \frac{1}{2}\mathbf{c})$ (*cf. International Tables for Crystallography*, 1995, Vol. A, ch. 15). Two parameter regions that can be mapped onto one another by this rotation necessarily correspond to the same sphere-packing type. The symbols of such regions are distinguished by an asterisk. If two parameter regions can be mapped onto one another by any other symmetry operation of $N_E(P6_122)$, their symbols differ by one or two primes.

Capital letters designate the centres of all those neighbour spheres that may have contact with a reference sphere with centre inside the parameter region of 3/10/*h*1 or on its boundaries. They are listed in Table 1. The sphere-packing types in the surroundings of 3/10/*h*1 are described in Table 2. The second column enumerates the symmetry operations

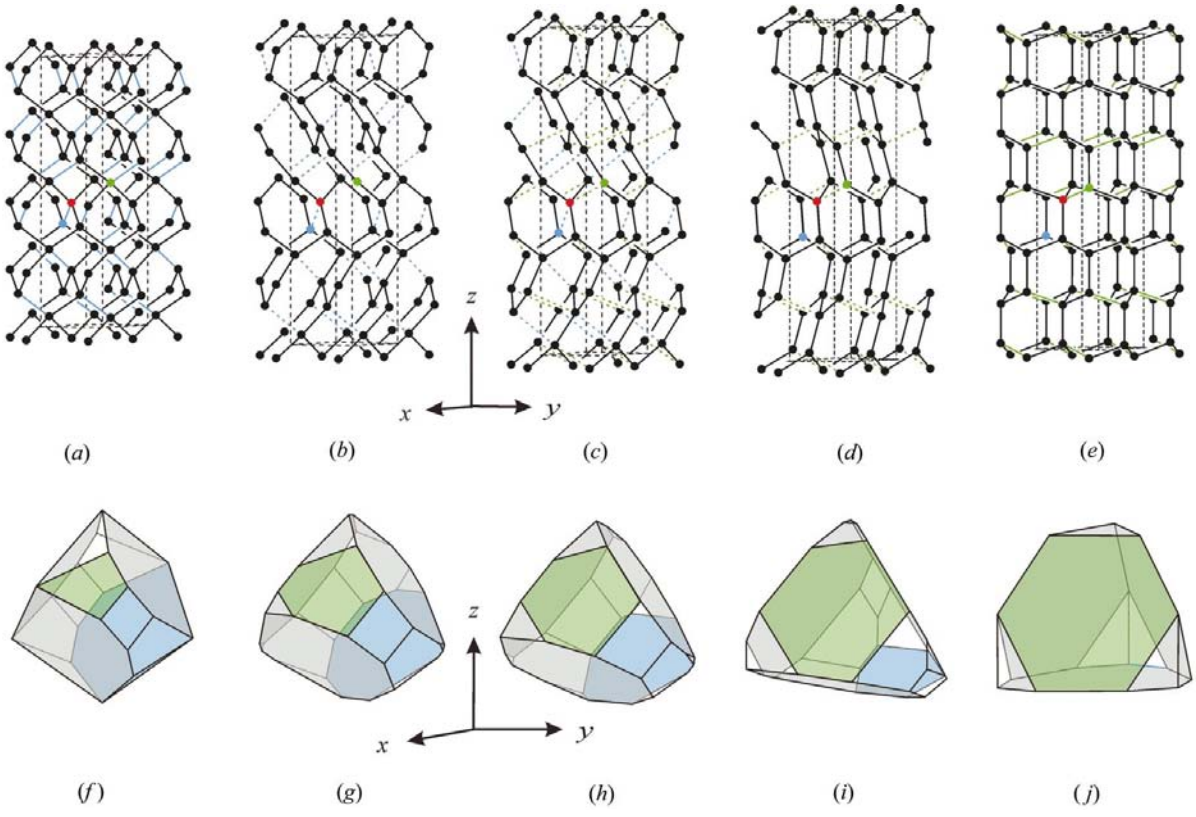


**Figure 3**
Sphere-packing deformations (*a*)–(*e*) and deformations of the corresponding Dirichlet domains (*f*)–(*j*) along the proposed transition path for different values of *x*. (*a*), (*f*) $x=\frac{1}{2}$, ideal arrangement of $\beta$-quartz; (*b*), (*g*) $x=\frac{19}{36}\approx 0.5278$; (*c*), (*h*) $x=\frac{5}{9}\approx 0.5556$; (*d*), (*i*) $x=\frac{11}{18}\approx 0.6111$; (*e*), (*j*) $x=\frac{2}{3}\approx 0.6667$, ideal arrangement of the high-temperature tridymite. Blue and green lines in (*a*)–(*e*) show the lost contacts in the ideal quartz and the ideal tridymite configuration, respectively. Accordingly, the blue and green coloured faces of the Dirichlet domains in (*f*)–(*j*) are caused by the lost neighbours.

**Table 2**
Sphere-packing types in the surroundings of 3/10/*h*1.

| | Neighbouring points | Additional conditions | Sphere-packing type | $\rho_{\min}$ | Maximal symmetry |
|---|---|---|---|---|---|
| 3.1 | *AB* | | 3/10/*h*1 | 0.25507 | $P6_222$ 6(*f*) |
| 2.1 | *ABC* | $y = 2x - \frac{1}{2}$ | 4/6/*h*1 | 0.39270 | $P6_422$ 3(*c*) |
| 2.2 | *ABD* | $x = \frac{2}{3}$ | 4/6/*h*2 | 0.34009 | $P6_3/mmc$ 4(*f*) |
| 2.3 | *ABE* | | 4/4/*h*4 | 0.33170 | $P6_222$ 6(*i*) |
| 2.4 | *ABF* | | 5/4/*h*7 | 0.47377 | $P6_122$ 12(*c*) |
| 2.5 | *ABG* | | 5/3/*h*3 | 0.44912 | $P6_122$ 12(*c*) |
| 2.6 | *ABH* | | 9/3/*h*3 | 0.64801 | $P6_222$ 6(*f*) |
| 1.1 | *ABEK* | $y = -x + \frac{1}{2}$ | 5/4/*h*6 | 0.51013 | $P6_422$ 3(*c*) |
| 1.1′ | *ABCE* | $y = 2x - \frac{1}{2}$ | | | |
| 1.2 | *ABCG* | $y = 2x - \frac{1}{2}$ | 6/3/*h*4 | 0.48934 | $P6_122$ 12(*c*) |
| 1.2′ | *ABCF* | $y = 2x - \frac{1}{2}$ | | | |
| 1.3 | *ABCJ* | $x = \frac{1}{3}$, $y = \frac{1}{6}$ | 5/3/*h*2 | 0.46271 | $P6_122$ 12(*c*) |
| 1.3′ | *ABCD* | $x = \frac{2}{3}$, $y = \frac{5}{6}$ | | | |
| 1.4 | *ABCH* | $y = 2x - \frac{1}{2}$ | 10/3/*h*3 | 0.69813 | $P6_422$ 3(*c*) |
| 1.5 | *ABDH* | $x = \frac{2}{3}$ | 10/3/*h*2 | 0.66568 | $P6_3/mmc$ 4(*f*) |
| 1.6 | *ABGJ* | $x = \frac{1}{3}$ | 6/3/*h*5 | 0.48107 | $P6_122$ 12(*c*) |
| 1.7 | *ABDE* | $x = \frac{2}{3}$ | 5/4/*h*5 | 0.40307 | $P6/mmm$ 2(*c*) |
| 1.8 | *ABDF* | $x = \frac{2}{3}$ | 6/3/*h*6 | 0.48107 | $P6_122$ 12(*c*) |
| 1.9 | *ABGK* | | 6/3/*h*7 | 0.47900 | $P6_122$ 12(*c*) |
| 1.9′ | *ABEF* | | | | |
| 1.10 | *ABEG* | | 6/3/*h*3 | 0.45821 | $P6_222$ 6(*i*) |
| 0.1 | *ABEKN* | $\frac{1}{2}$, 0, $\frac{3}{8}$, $\frac{3}{2} \times 2^{1/2}$ | 6/4/*h*3 | 0.51013 | $P6_422$ 3(*c*) |
| 0.1′ | *ABCEO* | $\frac{1}{2}$, $\frac{1}{2}$, $\frac{7}{24}$ | | | |
| 0.2 | *ABEGK* | 0.43670, 0.06330, 0.37079; 2.0697 | 7/3/*h*6 | 0.53633 | $P6_122$ 12(*c*) |
| 0.2′ | *ABCEG* | 0.43670, 0.37340, 0.29588 | | | |
| 0.2″ | *ABCEF* | 0.56330, 0.62660, 0.29588 | | | |
| 0.3 | *ABCGJ* | $\frac{1}{3}$, $\frac{1}{6}$, $\frac{1}{2} + (6^{1/2} - 3 \times 3^{1/2})/14$; 3.2080 | 7/3/*h*7 | 0.50736 | $P6_122$ 12(*c*) |
| 0.3′ | *ABCDF* | $\frac{2}{3}$, $\frac{5}{6}$, $\frac{1}{2} + (6^{1/2} - 3 \times 3^{1/2})/14$ | | | |
| 0.4 | *ABCHJ* | $\frac{1}{3}$, $\frac{1}{6}$, $1 - \frac{1}{2} \times 2^{1/2}$; $2 \times 6^{1/2} + 3 \times 3^{1/2}$ | 11/3/*h*1 | 0.71868 | $P6_122$ 12(*c*) |
| 0.4′ | *ABCDH* | $\frac{2}{3}$, $\frac{5}{6}$, $1 - \frac{1}{2} \times 2^{1/2}$ | | | |
| 0.5 | *ABGJK* | $\frac{1}{3}$, 0, $\frac{1}{3}$; $2 \times 2^{1/2}$ | 7/3/*h*8 | 0.49365 | $P6_122$ 12(*c*) |
| 0.5′ | *ABDEF* | $\frac{2}{3}$, $\frac{2}{3}$, $\frac{1}{3}$ | | | |

giving rise to sphere contacts. The third column shows some simple parameter conditions that must be fulfilled in addition to (1). Column 4 gives the symbol of the sphere-packing type and column 5 its minimal density $\rho_{\min}$. This quantity plays an important role for the assignment of the sphere packings to types. The last column displays the highest possible symmetry for a sphere packing of that type. Table 2 refers to only one half of the parameter field of 3/10/*h*1. All parameter regions in Fig. 2 marked by an asterisk are omitted.

## 4. The transition mechanism

As mentioned before, the ideal silicon arrangement in $\beta$-quartz corresponds to sphere-packing type 4/6/*h*1, which occurs *e.g.* at $x = y = \frac{1}{2}$, $z = \frac{7}{24}$ in $P6_122$ 12(*c*) with $c/a = 3 \times 2^{1/2} \simeq 4.2426$ (*cf.* Fig. 1). The neighbour points labelled *A*, *B* and *C* give rise to sphere contacts (2.1 in Table 2). In the undistorted tridymite configuration, which belongs to sphere-packing type 4/6/*h*2, the neighbours *A*, *B* and *D* yield sphere contacts (2.2). It is found at $x = \frac{2}{3}$, $y = \frac{1}{3}$, $z = \frac{5}{16}$ with $c/a = 2 \times 6^{1/2} \simeq 4.8990$. As the distances between adjacent Si atoms in $\beta$-quartz (*cf.* Kihara, 1990) and high-temperature tridymite (*cf.* Kihara, 1978) have almost the same length, for the following considerations the shortest distances are normalized to $d = 1$ and left constant during the entire transformation.

Starting from quartz, the sphere contact that corresponds to C is lost (and, of course, all symmetrically equivalent ones) resulting in a sphere packing of type 3/10/*h*1 (3.1). When the parameters of the ideal tridymite arrangement are reached, symmetry operation *D* yields again a fourth sphere contact. In principle, the transition path may be any one-dimensional route through the three-dimensional parameter region of 3/10/*h*1. In order to select a particular path, in addition to (1) two further parameter conditions must be chosen.

(i) The *a* lattice parameters of the high-temperature polymorphs of quartz ($a_q = 4.997$, $c_q = 5.455$ Å; Kihara, 1990) and tridymite ($a_t = 5.052$, $c_t = 8.270$ Å; Kihara, 1978) are very similar, whereas three times the *c* parameter of tridymite is about 13.7% longer than four times that of quartz. Therefore, it is suggested that *a* remains unchanged during the phase transition. Referred to a sphere diameter of 1, the lattice parameters of an idealized quartz configuration are $a_{qi} = \frac{2}{3} \times 6^{1/2} \simeq 1.6330$ and $c_{qi} = 4 \times 3^{1/2} \simeq 6.9282$ (referred to $P6_122$); those of an idealized tridymite configuration are $a_{ti} =$

$\frac{2}{3} \times 6^{1/2} \simeq 1.6330$ and $c_{ti} = 8$. Then, the ratio $c_{ti}/c_{qi} = 1.1547$ agrees quite well with that of the multiples of the $c$ parameters of quartz and tridymite. Therefore, as the first additional condition

$$a = \text{constant} = \tfrac{2}{3} \times 6^{1/2} \tag{2}$$

was chosen.

(ii) As the second additional condition,

$$y = 1 - x \tag{3}$$

was selected. As a consequence of (3), as many interatomic distances as possible become equal in length during the phase transition.

Equations (1), (2) and (3) together fix the transition path completely. Figs. 3(*a*)–(*e*) illustrate the sphere-packing deformations for some selected values of $x$. The three shortest distances within a sphere packing of type 3/10/*h*1 are drawn in black, the additional shortest distance within an ideal quartz or an ideal tridymite configuration is marked in blue or green, respectively. These two distances become equal at $x = \frac{5}{9} \approx 0.55556$ (Fig. 3*c*).

The sphere-packing deformation and the changes in the first and the second coordination shell are also reflected in the alterations of the corresponding Dirichlet domains (Figs. 3*f–j*). The Dirichlet domain of the ideal quartz configuration (Fig. 3*f*) is a truncated tetrahedron with 14 faces: four large hexagons, four triangles and four quadrangles of medium size, and two small quadrangles. All faces are caused by so-called direct neighbours, *i.e.* each line joining the central atom with one of these neighbours passes through the corresponding face. The Dirichlet domain of an ideal tridymite configuration (Fig. 3*j*) is a truncated tetrahedron with eleven faces: three large hexagons, one large nonagon and seven small triangles. Only the four large faces and one of the triangles are caused by direct neighbours. In Figs. 3(*f*)–(*j*), the three large faces that belong to the sphere-packing neighbours of 3/10/*h*1 are drawn in grey, whereas those faces that are related to the blue and green lines in Figs. 3(*a*)–(*e*) are coloured blue and green, respectively. The blue face develops from an edge of the tridymite polyhedron, quite similar to that previously described for the diamond–lonsdaleite transition (Sowa & Koch, 2001). The large green face of the tridymite polyhedron, however, originates from one of the medium-sized quadrangles of the quartz polyhedron.

Figs. 4 and 5 show the dependence of the coordinate $z$ and the lattice parameter $c$, respectively, on the $x$ coordinate.

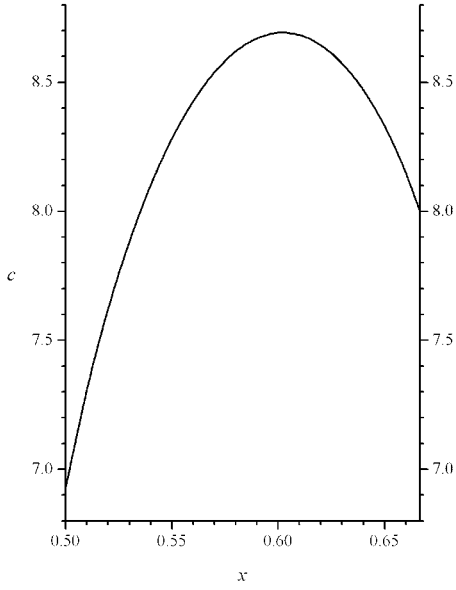


**Figure 5**
Variation of the lattice parameter $c$ depending on $x$ along the proposed transition path.

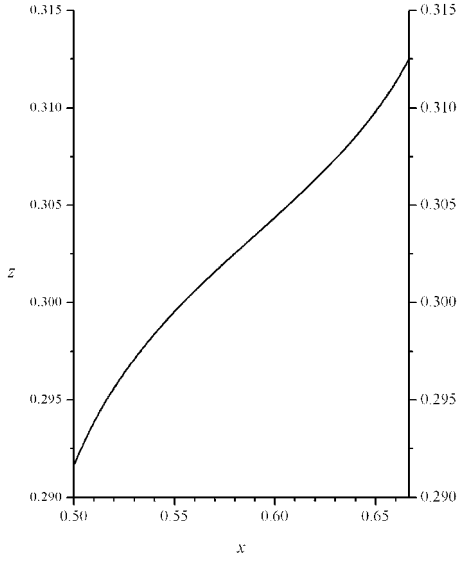


**Figure 4**
Variation of the coordinate $z$ depending on $x$ along the proposed transition path.

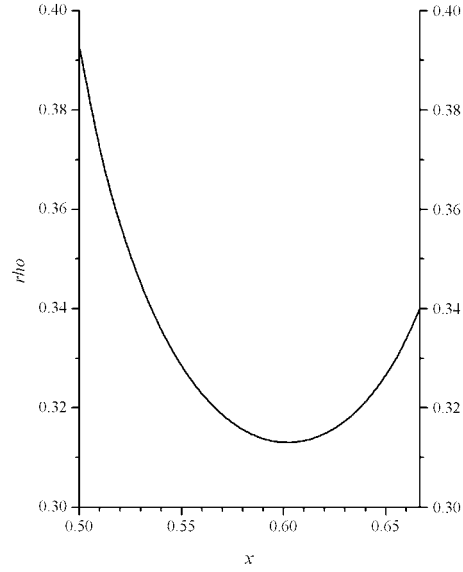


**Figure 6**
Variation of the sphere-packing density $\rho$ depending on $x$ along the proposed transition path.

Owing to (2), the axial ratio $c/a$ and the unit-cell volume $V$ show an analogous dependence on $x$ to $c$. Fig. 6 displays the variation of the sphere-packing density $\rho$ along the transition path. The changes of the distances between the original sphere and some neighbouring spheres during the phase transition are plotted in Fig. 7.

## 5. Discussion

In the present paper, a model for the transition between $\beta$-quartz and high-temperature tridymite is proposed that shows some interesting properties. During the whole transformation process, all silicon atoms remain symmetrically equivalent with respect to the common subgroup $P6_122$ of $P6_222$ and of $P6_3/mmc$.

The silicon atoms in the quartz structure are arranged in 12 layers perpendicular to **c** (referred to $P6_122$), and each silicon atom is connected *via* oxygen atoms with two silicon atoms from both neighbouring layers. During the phase transition, one of these four Si—O—Si links per Si atom must be removed. However, bonds are broken only between every other pair of Si layers and, for a certain pair of layers, all broken bonds run parallel (*cf.* Fig. 3*a*).

The three-dimensional connection of the crystal structure *via* Si—O—Si bonds is preserved during the entire transformation process, and the intermediate silicon arrangements give rise to sphere packings of type 3/10/*h*1 (Figs. 3*b–d*). This type is the hexagonal analogue (*cf.* Wells, 1975, p. 96; Koch & Fischer, 1995; O'Keeffe & Hyde, 1996, p. 298) of the tetragonal type of sphere packings 3/10/*t*4 (*cf.* Fischer, 1991), which corresponds to the silicon arrangement in $\alpha$-$ThSi_2$ (Koch, 1985). A sphere packing of type 3/10/*h*1 contains zigzag chains parallel to ⟨100⟩ arranged in double layers perpendicular to **c**. Six such double layers exist within one unit cell of $P6_122$, and all chains from a certain double layer run parallel. Each chain is alternately connected to a chain from the layers above and below. In the quartz structure, each zigzag chain lies in a plane parallel to **c**. During the transition, each chain is rotated around its middle axis without any deformation (*cf.* Figs. 3*a–e*). As a consequence, the distance *between* the two nearest neighbours labelled *A* in Table 1 does not change along the entire transition path, *i.e.* $d_{AA} = 3^{1/2}$. In the tridymite structure, the silicon atoms also form 12 layers perpendicular to **c** but, in contrast to quartz, each silicon atom is connected *via* one Si—O—Si bond to the first neighbouring layer and *via* three such bonds to the other.

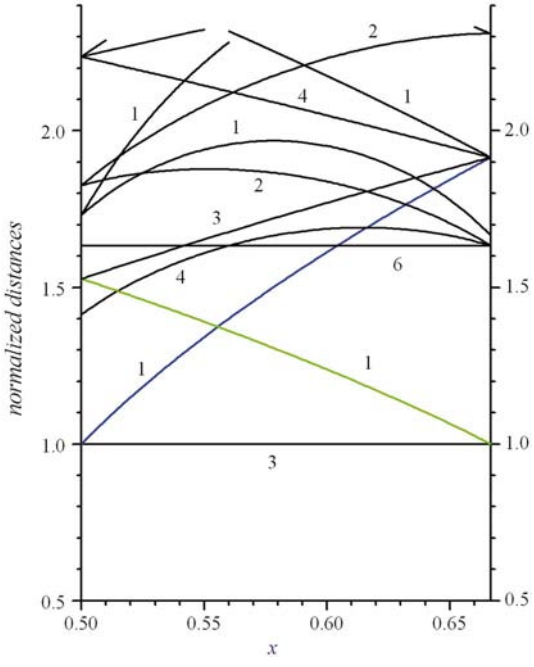


**Figure 7**
Variations of the interatomic distances depending on $x$ along the proposed transition path. The blue and the green lines mark the distance from the central sphere to the lost neighbour in the ideal quartz and in the ideal tridymite configuration, respectively.

At a certain point in the course of the transition, namely for $x = \frac{5}{9}$, $y = \frac{4}{9}$, $z = 0.30013$ and $c/a = 5.1234$, the two next nearest neighbours (labelled *C* and *D* in Table 1) are equidistant from the central atom (*cf.* Figs. 3*c* and 6). They are located at different sides of the almost isosceles triangle formed by the three nearest neighbours, and their distances are only 37% longer than the shortest three. One of these two neighbours originates from the first coordination shell in the quartz structure ($x = \frac{1}{2}$), the other one gives rise to the newly formed bonds in the tridymite structure ($x = \frac{2}{3}$). At $x = \frac{5}{9} \simeq 0.55556$, each atom lies nearly (but not exactly) in the same plane with its three nearest neighbours. The sphere-packing density amounts to $\rho = 0.32519$, whereas the minimal density for type 3/10/*h*1 is only $\rho_{min} = 0.25507$ (Koch & Fischer, 1995). It is found at $x = \frac{1}{2}$, $y = 0$, $z = \frac{5}{16}$ and $c/a = 3 \times 2^{1/2} \simeq 4.2426$. O'Keeffe & Hyde (1996, p. 298) presented a sphere packing of this type with all angles being 120°. Its density is $\rho = 0.26871$. Within the present parameter field, it occurs at $x = \frac{1}{2}$, $y = 0$, $z = \frac{11}{36} \simeq 0.30556$ and $c/a = 3 \times 3^{1/2} \simeq 5.1962$. For the proposed transition path, the first coordination shell is entirely flat at $x = 0.57834$ ($\rho = 0.31606$). This parameter corresponds neither to the sphere packing with minimal density nor to that with all angles being 120°.

The proposed transition model is diffusionless, *i.e.* only relatively small cooperative movements of the atoms are necessary. It results in a parallel orientation of the hexagonal unit cells of quartz and tridymite.

For the migration of the oxygen atoms, Leoni & Nesper (2000) have proposed a two-O-atom four-centre transition path. The present paper only describes the movement of the silicon atoms under preservation of the symmetry $P6_122$. If one wants to regard in addition the migration of the oxygen atoms, reduction of the symmetry to the translational-equivalent subgroup $P6_1$ of $P6_122$ is necessary. Here, the 12 silicon atoms per unit cell split into two symmetrically different kinds. In tridymite as well as in quartz, each Si atom of one kind has four neighbouring atoms of the other kind and *vice versa*, *i.e.* each oxygen atom connects two silicon atoms of different kind. All O atoms belonging to the breaking bonds in the Si net are symmetrically equivalent in $P6_1$. During the

phase transition, they may remain, for instance, near the Si atoms of the first kind, whereas the Si atoms of the second kind have only three nearest O neighbours and interchange the fourth one.

The calculations of Leoni & Nesper (2000) also result in an intermediate arrangement between the high-temperature polymorphs of quartz and tridymite with a 3-coordinated silicon network. The authors compared this arrangement with the configuration of the B atoms in $B_2O_3$, which form a distorted heterogeneous sphere packing with symmetry $P3_1$. As has been already mentioned by O'Keeffe & Hyde (1996, p. 298), this heterogeneous sphere packing corresponds to a homogeneous one of type 3/10/*h*1. O'Keeffe & Hyde, however, ascribed $P3_112$ as maximal possible symmetry to this type instead of $P6_422$ or $P6_222$.

At a first glance, the intermediate structure proposed by Leoni & Nesper (2000) seems to be very similar to that described in the present paper. Leoni & Nesper, however, claim the intermediate symmetry is only $P2_1$. Their calculations should result in an intermediate space group which is an intersection group of the space groups of the high-temperature phases of tridymite and quartz with parallel oriented unit cells, *i.e.* of $P6_3/mmc$ and of $P6_222$ or $P6_422$. Furthermore, $a(P6_3/mmc) = a(P6_222)$ and $3c(P6_3/mmc) = 4c(P6_222)$ must hold. The intersection group, however, is not unique but depends on the relative origin choices for the unit cells of tridymite and quartz, *i.e.* on the phases of the reflections chosen for the calculation of the periodic equi-surfaces. The origin choice for quartz and tridymite that is used in the present paper results in $P6_3/mmc$ (3**c**) $\cap$ $P6_222$ (4**c**) = $P6_522$ or in $P6_3/mmc$ (3**c**) $\cap$ $P6_422$ (4**c**) = $P6_122$. Other choices may yield *e.g.* $P6_5$ or $P6_1$, $C222_1$, $C2$, $P2_1$ or even $P1$. An intermediate space group $P2_1$ as reported by Leoni & Nesper (2000) corresponds to a mutual origin shift, *e.g.* by $(\frac{1}{2}, 0, z)$.

Orientation relations between high-temperature tridymite and $\beta$-quartz seem to be discussed very rarely. Ray (1947) studied quartz paramorphs after tridymite from Home, Colorado, USA. He found that the optic axis of quartz deviates from the direction normal to the basal face of the former tridymite crystals in a range between 14 and 83° with an average of about 61°, which 'might mean that the $(10\bar{1}1)$ face of tridymite has become the (0001) of quartz'. Flörke (1959) also investigated quartz paramorphs after tridymite from the Euganean Hills, Italy. His measurements of the respective angle accumulated in a value of 52° but also spread over a wide range. Both results are not compatible with the model discussed in the present paper. Nevertheless, it seems to be not unlikely that the proposed transition mechanism may be realized under specific conditions because of the very short migration paths of all atoms.

## References


Fischer, W. (1971). *Z. Kristallogr.* **133**, 18–42.
Fischer, W. (1991). *Z. Kristallogr.* **194**, 67–85.
Fischer, W. & Koch, E. (1994). *Z. Kristallogr.*, Suppl. No. 9, p. 208.
Flörke, O. W. (1959). *Z. Kristallogr.* **112**, 126–135.
Flörke, O. W. & Langer, K. (1972). *Contrib. Mineral. Petrol.* **36**, 221–230.
*International Tables for Crystallography* (1995). Vol. A, edited by Th. Hahn. Dordrecht/Boston/London: Kluwer Academic Publishers.
Kihara, K. (1978). *Z. Kristallogr.* **148**, 237–253.
Kihara, K. (1990). *Eur. J. Mineral.* **2**, 63–77.
Koch, E. (1985). *Z. Kristallogr.* **173**, 205–224.
Koch, E. & Fischer, W. (1995). *Z. Kristallogr.* **210**, 407–414.
Leoni, S. & Nesper, R. (2000). *Acta Cryst.* A**56**, 383–393.
O'Keeffe, M. & Hyde, B. G. (1996). *Crystal Structures.* Washington: Mineralogical Society of America.
Putnis, A. (1992). *Introduction to Mineral Sciences.* Cambridge University Press.
Ray, L. L. (1947). *Am. Mineral.* **32**, 643–646.
Schnering, H. G. von & Nesper, R. (1991). *Z. Phys. B*, **83**, 407–412.
Sowa, H. (2001). *Acta Cryst.* A**57**, 176–182.
Sowa, H. & Koch, E. (2001). *Acta Cryst.* A**57**, 406–413.
Wells, A. F. (1975). *Structural Inorganic Chemistry*, 4th ed. Oxford: Clarendon Press.